

ICONE  
Conference Paper

American Society of Mechanical Engineers (ASME) owns all copyright and publication subject to this requirement: "Verbatim reproduction of this paper by anyone will be permitted by ASME provided appropriate credit is given to the author(s) and ASME."

## ICONE 10-22292

### FEASIBILITY OF NATURAL CIRCULATION HEAT TRANSPORT IN THE ENHS

James J. Sienicki  
Argonne National Laboratory  
9700 South Cass Avenue  
Argonne, Illinois 60439, USA  
email: sienicki@anl.gov

**KEYWORDS:** Generation IV, Advanced Reactors, Heavy Liquid Metal Coolant, Lead-Bismuth Eutectic, Natural Convection

#### ABSTRACT

An analysis has been carried out of natural circulation thermal hydraulics in both the primary and intermediate circuits of the Encapsulated Nuclear Heat Source (ENHS). It is established that natural circulation enhanced by gas injection into the primary coolant above the core, or the intermediate coolant above the heat exchange zone, is effective in transporting the nominal core power to the steam generators without the attainment of excessive system temperatures. Uncertainties in thermophysical properties and wall friction have a relatively small effect upon the calculated best estimate primary and intermediate coolant system temperature rises.

#### INTRODUCTION

The Encapsulated Nuclear Heat Source (ENHS) is a small innovative reactor concept of 125 MWt/50 MWe.<sup>1-3</sup> The fuel is “encapsulated” inside a removable cylindrical primary coolant vessel through out the 20-year core life restricting access to fuel and neutrons (Figure 1). The ENHS utilizes lead-bismuth eutectic (55 wt% Bi-45 wt% Pb;  $T_{\text{melt}} = 125\text{ }^{\circ}\text{C}$ ;  $T_{\text{boil}} = 1670\text{ }^{\circ}\text{C}$ ) or lead ( $T_{\text{melt}} = 327\text{ }^{\circ}\text{C}$ ;  $T_{\text{boil}} = 1740\text{ }^{\circ}\text{C}$ ) heavy liquid metal coolant (HLMC). These coolants do not react exothermically or vigorously with water or steam, and do not burn when exposed to air.

The reactor concept relies upon heat transport by natural circulation of both the primary and intermediate heavy liquid metal coolants. There are no mechanical main circulation pumps in the primary or secondary circuits. Primary-to-intermediate coolant heat exchange takes place inside an annular heat exchanger (HX) region inside the primary coolant vessel (Figure 2). In the reference design, intermediate coolant flows upward through long aspect ratio thick-walled parallel plate channels while primary coolant flows downward over the

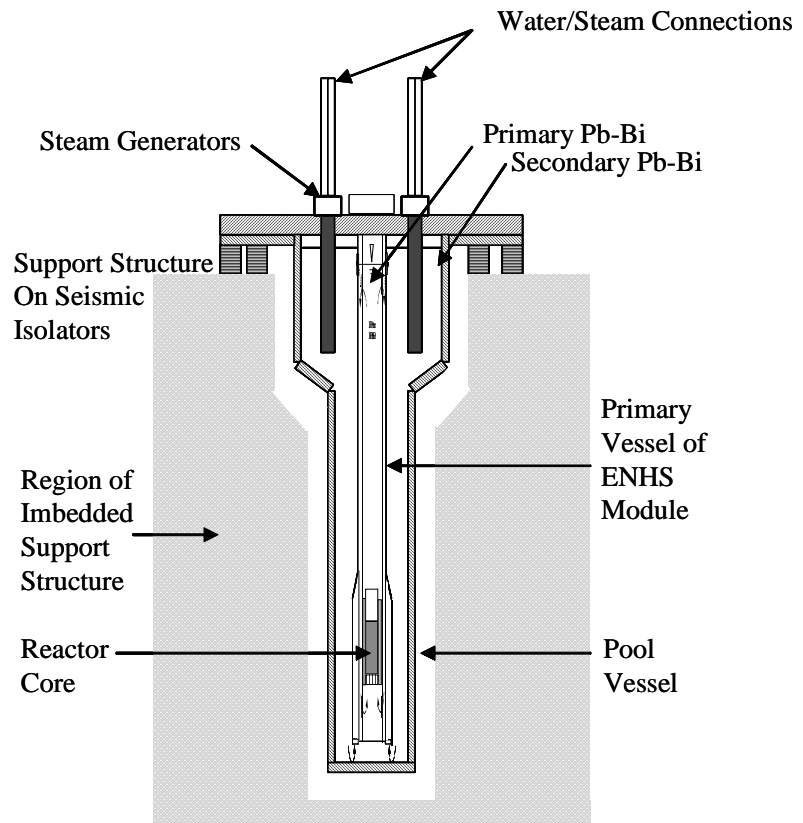


Figure 1. Illustration of Possible ENHS Concept.

plate exterior surfaces. The removable ENHS primary coolant vessel is placed inside an annular intermediate coolant pool. Heat exchange between the intermediate coolant and the water/steam working fluid occurs inside modular steam

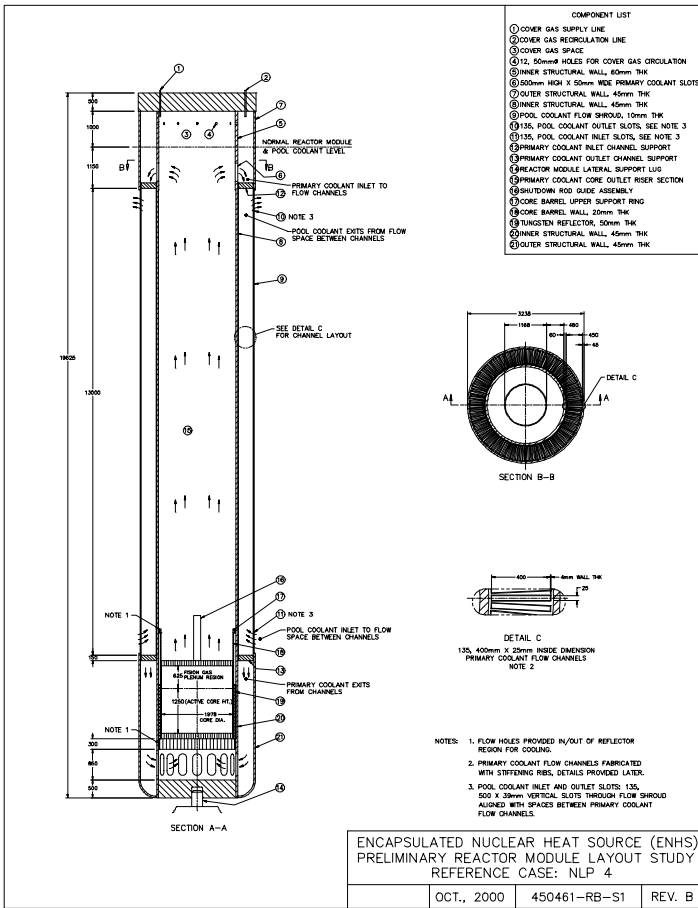


Figure 2. Illustration of ENHS Primary Coolant Heat Exchanger Regions for NLP4 Design Variant.

generators (SGs) located near the top of the annular intermediate coolant pool. The intermediate coolant flows downward over numerous tube-in-tube channels inside which water enters flowing downward through the central tube and steam exits flowing upward through the annulus. If needed, the ENHS optionally incorporates the injection of noncondensable gas (i.e., a lift pump) into the primary coolant above the core or into the intermediate coolant above the HX plate channels (Figure 3) to enhance the coolant flowrate above that from single-phase natural circulation alone.

The ENHS is not a single design; a number of different design variants have been specified based upon absence or incorporation of a lift pump as well as variations in the core, riser, HX, and SG dimensions.

The objectives of the present work are to: i) establish the feasibility of natural circulation heat transport for both primary and intermediate circuits; and ii) determine the effects of uncertainties inherent in lead-bismuth eutectic (LBE) and lead thermophysical properties as well as the representation of wall friction. The approach consists of development of a mainly analytical model for natural circulation flows and heat transfer through the application of first principles modeling to the ENHS design. The present work models natural circulation

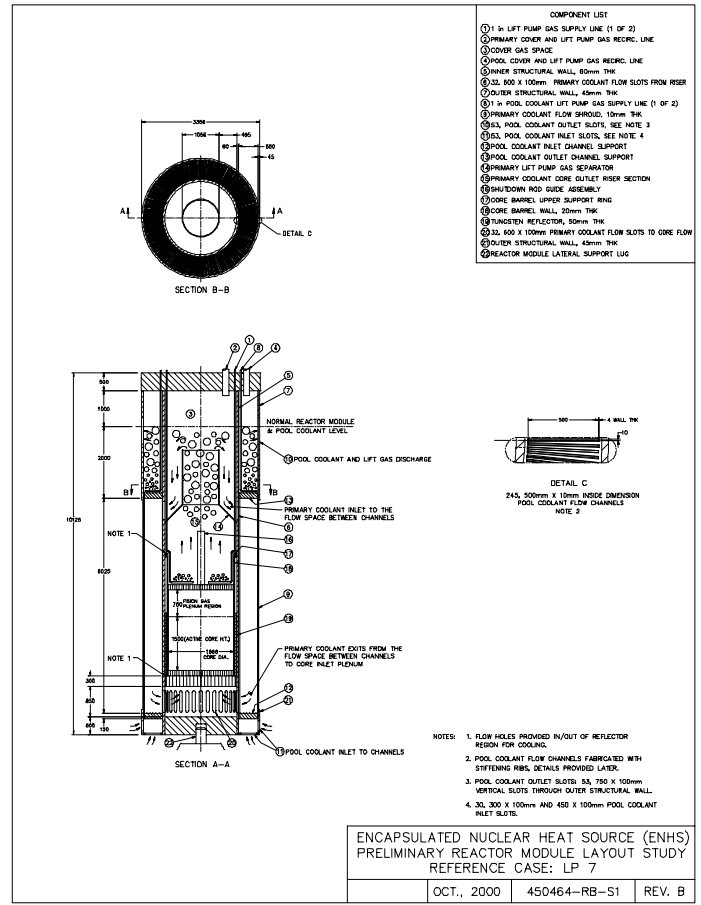


Figure 3. Illustration of ENHS Primary Coolant and Heat Exchanger Regions for LP7 Design Variant.

flow and heat transfer of both the primary and intermediate coolants together in a single integrated and refined framework, whereas previous analyses<sup>4</sup> addressed only the primary coolant system while treating the intermediate coolant through boundary conditions that were at best approximate.

## NOMENCLATURE

- A = flow area, m<sup>2</sup>
- c = specific heat, J/(Kg•K)
- D<sub>h</sub> = hydraulic diameter, m
- F = frictional term
- f = friction factor
- g = gravitational acceleration, m/s<sup>2</sup>
- H = inverse thermal resistance, W/(m<sup>2</sup>•K)
- h = heat transfer coefficient from primary bulk coolant, W/(m<sup>2</sup>•K)
- h<sub>i</sub> = heat transfer coefficient to intermediate bulk coolant, W/(m<sup>2</sup>•K)
- K = frictional loss coefficient
- k = thermal conductivity, W/(m•K)
- k<sub>s</sub> = grainsize for roughness, m

$k_{wall}$	=	thermal conductivity of HX plate wall W/(m•K)
$L_{cooled}$	=	length for frictional losses associated with cooled zone, m
$L_{diff}$	=	difference in elevation between cooled and heated zone thermal centers, m
$L_{heated}$	=	length for frictional losses associated with heated zone, m
$L_{2\phi}$	=	height of two-phase region, m
$Nu$	=	$\frac{hD_h}{k}$ = Nusselt number
$Pr$	=	$\frac{c\mu}{k}$ = Prandtl number
$Q_{tot}$	=	total reactor power, W
$R_h$	=	hydraulic radius, m
$Re$	=	$\frac{\rho u D_h}{\mu}$ = Reynolds number
$S$	=	perimeter, m
$T$	=	temperature, K
$T_{in}$	=	inlet temperature, K
$T_{out}$	=	outlet temperature, K
$u$	=	primary coolant velocity, m/s
$u_{heated}$	=	velocity through heated zone, m/s
$u_i$	=	intermediate coolant velocity, m/s
$x$	=	$\frac{1}{2f^{1/2}}$
$\bar{x}$	=	position vector, m
$z$	=	vertical coordinate directed downwards, m

### Greek Letters

$\alpha_{2\phi}$	=	void fraction of gas,
$\beta$	=	$-\frac{1}{\rho} \frac{d\rho}{dT}$ = compressibility/thermal expansion coefficient, K <sup>-1</sup>
$\Delta T$	=	temperature rise through heated zone, K
$\delta_{wall}$	=	wall thickness, m
$\epsilon_M$	=	turbulent eddy diffusivity of momentum, m <sup>2</sup> /s
$\mu$	=	viscosity, Kg/(m•s)
$\nu$	=	$\mu/\rho$
	=	kinematic viscosity, m <sup>2</sup> /s
$\rho$	=	density, Kg/m <sup>3</sup>
$\bar{\rho}$	=	coolant physical/liquid density evaluated at mean coolant temperature, Kg/m <sup>3</sup>
$\rho_\ell$	=	coolant liquid density at core outlet temperature, Kg/m <sup>3</sup>
$\bar{\Psi}$	=	average effective eddy diffusivity ratio

### Subscripts

$i$	=	heated intermediate coolant
-----	---	-----------------------------

### ANALYSIS APPROACH

Steady state heavy liquid metal coolant flow and temperature conditions are calculated with a one-dimensional formulation. An equation is derived for the quasi-steady coolant velocity through the primary or intermediate circuit heated zone. The Bernoulli form of the steady state one-dimensional momentum equation is integrated over a closed circuit. The effective driving pressure rise from buoyancy due to single-phase temperature differences is

$$\oint \rho \bar{g} \cdot d\bar{x} = \oint (\rho - \bar{\rho}) \bar{g} \cdot d\bar{x} = \bar{\rho} g \beta (T_{out} - T_{in}) L_{diff}. \quad (1)$$

The enhancement in driving head due to buoyancy from noncondensable gas injection above the heated zone is

$$(\rho_\ell - \rho_{2\phi}) g L_{2\phi} \approx \rho_\ell \alpha_{2\phi} g L_{2\phi} = \bar{\rho} \left( 1 - \frac{\beta \Delta T}{2} \right) \alpha_{2\phi} g L_{2\phi}. \quad (2)$$

The temperature rise across the heated zone from energy conservation is

$$\Delta T = T_{out} - T_{in} = \frac{Q_{tot}}{\bar{\rho} u_{heated} A_{heated} c}. \quad (3)$$

Using this equation to eliminate the core temperature rise provides an equation for the velocity through the heated zone in terms of total power,

$$u_{heated} = \left[ \frac{Q_{tot} g \beta \left( L_{diff} - \frac{\alpha_{2\phi} L_{2\phi}}{2} \right) + \frac{g \alpha_{2\phi} L_{2\phi} u_c}{2}}{2 \bar{\rho} c A_{heated}} \right]^{1/3} \times \left[ \frac{L_{heated}}{D_{h,heated}} \left( f_{heated} + \frac{\sum K_{i,heated} D_{h,heated}}{4 L_{heated}} \right) + \left( \frac{A_{heated}}{A_{cooled}} \right)^2 \frac{L_{cooled}}{D_{h,cooled}} \left( f_{cooled} + \frac{\sum K_{i,cooled} D_{h,cooled}}{4 L_{cooled}} \right) \right]^{-1/3}. \quad (4)$$

The model employs the turbulent friction factor of Colebrook and White<sup>5</sup> that depends upon a grain size for roughness,

$$f = \frac{1}{4x^2}, \quad (5)$$

$$x = 1.74 + \frac{2}{\ln 10} \ln \left( \frac{k_s}{R_h} + \frac{18.7x}{Re} \right). \quad (6)$$

A roughness size of 10 microns is nominally assumed as representative of an oxide film.

The model incorporates an analytical solution of one-dimensional equations for primary and intermediate bulk coolant temperatures along the height of the heat exchanger,

$$\rho u A c \frac{dT}{dz} = -HS(T - T_i), \quad (7)$$

$$-\rho_i u_i A_i c_i \frac{dT_i}{dz} = HS(T - T_i). \quad (8)$$

The inverse thermal resistance between primary and intermediate bulk coolants is

$$H = \frac{1}{\frac{1}{h} + \frac{\delta_{wall}}{k_{wall}} + \frac{1}{h_i}}. \quad (9)$$

The correlation of Dwyer<sup>6</sup> for liquid metal heat transfer from parallel plates for identical heat fluxes from both plate walls is assumed for both the primary and intermediate coolant forced convection heat transfer coefficients,

$$Nu = 9.49 + 0.0596(\bar{\Psi} Re Pr)^{0.688}. \quad (10)$$

The average effective eddy diffusivity ratio is given by the semiempirical equation proposed by Dwyer,<sup>6</sup>

$$\bar{\Psi} = 1 - \frac{1.82}{Pr \left( \frac{\epsilon_M}{v} \right)_{max}^{1.4}}. \quad (11)$$

The following function was fit to the figure of Dwyer<sup>6</sup> presenting  $(\epsilon_M / v)_{max}^{1.4}$  versus Reynolds number for the case of concentric annuli,

$$\left( \frac{\epsilon_M}{v} \right)_{max}^{1.4} = 7.833 \times 10^{-4} Re^{1.2}. \quad (12)$$

Although a protective oxide layer is present at the channel walls, the assumed 10 micron nominal thickness is too small to contribute a significant thermal resistance relative to the calculated forced convection heat transfer coefficients. The level of dissolved oxygen in the melt is assumed to be controlled to maintain the oxide layer and minimize the presence of contaminants in the coolant. Thus, no additional thermal resistance is assumed due to an oxide layer or contaminants at the channel walls.

Four ENHS design variants were analyzed. Detailed design conditions are shown in Table 1. Case NLP4 (No Lift Pump Case No. 4) incorporates the greatest riser heights above the core and HX (Figure 2) to enhance single-phase natural circulation from coolant temperature differences alone. Case LP6 (Lift Pump Case No. 6) includes enhanced circulation from gas injection with somewhat reduced riser heights. Case LP7

features a compact design with gas injection and significantly reduced riser heights above both the core and HX (Figure 3). A fourth variant of LP7 extends the bottom of the HX that was located completely above the core down to the active core lower elevation. The single constraint upon the temperatures in the calculations is that the primary coolant inlet temperature at the bottom of the core equals 400 °C.

The analysis uses temperature dependent thermophysical properties for LBE and lead evaluated at the mean of the primary and intermediate coolant outlet and inlet temperatures. The properties were determined by members of the ENHS Project Team and are being used consistently in all ENHS analyses.

## FINDINGS

Table 2 shows the results calculated for each case with the alternative choices of LBE and lead coolants. The major figures of merit are the primary and intermediate coolant temperature rises across the respective heated zones. It is desired that the temperature rises remain less than about 160 C. This limits the coolant outlet temperatures to values of 560 C or less for which it is expected that ferritic steels such as HT9 could be used as a structural material together with the formation and maintenance of a corrosion-inhibiting oxide layer on the structural wall surface.

The calculated heated zone temperature rises for the primary and intermediate coolants all meet the figures of merit such that reliance upon pure or gas-injection augmented natural circulation of the primary and intermediate coolants is effective in transporting the nominal core power from the fuel rods to the HX as well as from the HX to the steam generators. As observed from Table 2, very small differences in the results are calculated between LBE and lead coolants.

Effects of uncertainties in the LBE and lead coolant thermophysical properties were examined. Variations in thermophysical properties that cause  $\Delta T$  to increase are of present interest. Under pure natural circulation (i.e., no gas injection), the coolant velocity through the heated zone is given by

$$u_{heated} = \left( \frac{Qg\beta L_{diff}}{2\rho c A F} \right)^{1/3} \quad (13)$$

such that the temperature rise across the heated zone is

$$\Delta T = \frac{Q}{\rho c u_{heated} A} = \left( \frac{Q}{\rho c A} \right)^{2/3} \left( \frac{2F}{g\beta L_{diff}} \right)^{1/3}. \quad (14)$$

Thus, an increase in  $\Delta T$  will result from decreases in  $\beta$ ,  $\rho$ , and  $c$  as well as from an increase in  $F$ . The present approach consists of decreasing  $\beta$ ,  $\rho$ ,  $c$ , and  $k$  while increasing the viscosity,  $\mu$ , consistent with data uncertainties or scatter for the variables in

Table 1. Comparison of ENHS Design Variants.

<b>Design</b>	<b>NLP4</b>	<b>LP6</b>	<b>LP7</b>	<b>LP7 with HX Extending to Bottom of Active Core</b>
Gas Injection Above Core and HX	No	Yes	Yes	Yes
Heated Core/Fission Gas Plenum Height, m	1.25/0.625	1.25/0.625	0.933	0.933
Core Radius, m	0.989	0.788	0.933	0.933
Fuel Rod Diameter, cm	1.20	.20	1.20	1.20
Rod Pitch-to-Diameter Ratio	1.208	1.108	1.247	1.247
Riser/HX Channel Heights, m	13/11	10/8	3.0/1.75	3.0/3.25
HX Channel Thickness/Width, cm	2.5/40	1.7/40	0.5/50	0.5/50
HX Channel Wall Thickness, cm	0.4	0.4	0.4	0.4
SG Heat Exchange Height, m	4.6	4.6	4.6	4.6
Number of SG Modules/Tubes per Module	8/613	8/613	8/613	8/613
Primary/Intermediate Two-Phase Region Height	0/0	8/2	1.75/2	1.75/2
Void Fraction	0.0	0.1	0.1	0.1
Primary Coolant Core/HX Hydraulic Diameter, cm	0.732/4.41	0.425/3.14	0.856/1.00	0.856/1.00
Intermediate Coolant HX/SG Hydraulic Diameter, cm	4.71/2.51	3.26/2.51	0.990/2.51	0.990/2.51

Table 2. ENHS Thermal Hydraulic Conditions.

<b>Design</b>	<b>NLP4</b>	<b>LP6</b>	<b>LP7</b>	<b>LP7 with HX Extending to Bottom of Active Core</b>
Coolant	LBE/Lead	LBE/Lead	LBE/Lead	LBE/Lead
Gas Injection Above Core/Lift Pump	No	Yes	Yes	Yes
Primary Coolant Velocity in Core, m/s	0.515/0.492	1.08/1.06	0.600/0.582	0.479/0.466
Primary Coolant Velocity in HX, m/s	0.384/0.366	0.446/0.436	0.552/0.536	0.441/0.429
Intermediate Coolant Velocity in HX, m/s	0.447/0.426	0.795/0.776	0.725/0.710	0.604/0.589
Intermediate Coolant Velocity in SG, m/s	0.294/0.281	0.414/0.404	0.384/0.376	0.320/0.312
Primary Coolant Temperature Rise, °C	145/147	158/157	127/127	160/160
Intermediate Coolant Temperature Rise, °C	139/141	99.0/98.2	107/105	129/128
Primary Coolant Outlet Temperature, °C	545/547	558/557	527/527	560/560
Intermediate Coolant Temperature at Top of HX, °C	497/502	479/480	477/478	519/519
Intermediate Coolant Temperature at Bottom of HX	358/360	380/382	370/372	390/391
Primary-to-Intermediate Coolant Temperature Difference at Top of HX, °C	47.8/45.6	78.8/76.9	50.5/49.8	41.1/41.0
Primary-to-Intermediate Coolant Temperature Difference at Bottom of HX, °C	42.4/39.6	19.7/17.8	29.9/27.6	9.62/8.87

Table 3. Effects of Uncertainties in LBE Thermophysical Properties for NLP4.

<b>Case Designation</b>	<b>NLP4</b>	<b>NLP4 with Density and Compressibility of Nikol'skii et. al.</b>	<b>NLP4 with Density and Compressibility of Nikol'skii et. al. Also Decrease Density by 1.5%, Specific Heat by 1%, Thermal Conductivity by 3%; Increase Viscosity by 6%</b>
Primary Coolant Velocity in Core, m/s	0.515	0.491	0.494
Primary Coolant Velocity in HX, m/s	0.384	0.366	0.368
Intermediate Coolant Velocity in HX, m/s	0.447	0.426	0.429
Intermediate Coolant Velocity in SG, m/s	0.294	0.281	0.282
Primary Coolant Temperature Rise, °C	145	151	154
Intermediate Coolant Temperature Rise, °C	139	145	148
Primary Coolant Outlet Temperature, °C	545	551	554
Intermediate Coolant Temperature at Top of HX, °C	497	502	505
Intermediate Coolant Temperature at Bottom of HX, °C	358	357	356
Primary-to-Intermediate Coolant Temperature Difference at Top of HX, °C	47.8	48.4	49.3
Primary-to-Intermediate Coolant Temperature Difference at Bottom of HX, °C	42.4	42.8	43.5

Table 4. Effects of Uncertainties in Lead Thermophysical Properties for NLP4.

<b>Case Designation</b>	<b>NLP4</b>	<b>NLP4 with Density and Compressibility of Crawley</b>	<b>NLP4 with Density and Compressibility of Crawley. Also Decrease Density by 0.5%, Specific Heat by 1.6%, Thermal Conductivity by 6%; Increase Viscosity by 3%</b>
Primary Coolant Velocity in Core, m/s	0.492	0.477	0.479
Primary Coolant Velocity in HX, m/s	0.366	0.355	0.357
Intermediate Coolant Velocity in HX, m/s	0.426	0.413	0.416
Intermediate Coolant Velocity in SG, m/s	0.281	0.272	0.274
Primary Coolant Temperature Rise, °C	147	153	155
Intermediate Coolant Temperature Rise, °C	141	147	149
Primary Coolant Outlet Temperature, °C	547	553	555
Intermediate Coolant Temperature at Top of HX, °C	502	507	508
Intermediate Coolant Temperature at Bottom of HX, °C	360	360	359
Primary-to-Intermediate Coolant Temperature Difference at Top of HX, °C	45.6	46.1	47.5
Primary-to-Intermediate Coolant Temperature Difference at Bottom of HX, °C	39.6	40.0	41.3

those directions. The results are shown in Tables 3 and 4 for LBE and lead coolants, respectively.

The most significant uncertainties involves the volume thermal expansion coefficient/compressibility,  $\beta$ . In order to separately quantify the effects of uncertainties in  $\beta$ , variations in the properties were carried out in two steps. The first involves variation in only the density and compressibility. The density and compressibility of LBE are nominally assumed given by the equation of Been, Edwards, Teeter, and Calkins,<sup>7</sup>

$$\rho = 10740 - 1.38(T - 273.15), \quad (15)$$

selected by the ENHS team. That equation is replaced with the equation recommended by Nikol'skii, Kalakutskaya, Pchelkin, Klassen, and Vel'tischeva,<sup>8</sup>

$$\rho = 10730 - 1.22(T - 273.15). \quad (16)$$

The rationale is that the Nikol'skii et. al. equation provides a significantly lower compressibility,  $\beta$ .

In addition to the first variation, the second variation also performs the following changes:

<u>Change</u>	<u>Rationale</u>
Decrease density by 1.5%	Uncertainty in density reported by Been et. al. is $\pm 1.5\%$
Decrease c by 1%	Curve used by ENHS team lies below other data. Round off error of 1% is made in literature
Decrease k by 3%	Data points lying below curve used by ENHS team
Increase $\mu$ by 6%	Uncertainty assessed by Fink <sup>9</sup> is $\pm 6\%$

It is observed from Table 3 that uncertainties in  $\beta$  alone could raise the heated zone temperature rises by 6 °C above the values in Table 3. Additional property uncertainties could further increase the heated zone temperature rises to a total of 9 C.

For lead coolant, the nominal density and compressibility selected by the ENHS team are given by the equation of Saar and Ruppertsberg,<sup>10</sup>

$$\rho = 10600 - 1.35(T - 600). \quad (17)$$

Their equation is replaced with that recommended by Crawley,<sup>11</sup>

$$\rho = 15870 - 1.222(T - 600.6), \quad (18)$$

that provides a significantly lower compressibility. In addition to this variation, the second variation also makes the following changes:

<u>Change</u>	<u>Rationale</u>
Decrease density by 0.5%	Uncertainty in density reported by Saar and Ruppertsberg is $\pm 0.5\%$
Decrease c by 1.6%	Uncertainty at 1000 K according to Fink <sup>12</sup>
Decrease k by 6%	Data points lying below curve used by ENHS team
Increase $\mu$ by 3%	Data points lying above curve used by ENHS team

It is observed from Table 4 that the possible increases in the heated zone temperature rises with lead coolant are similar to those for LBE.

Table 5. Effects of Roughness Grain Size for NLP4 with LBE Coolant.

Roughness Grain Size, $\mu\text{m}$	0.01	0.1	1.0	10	50	100	1000
Primary Coolant Velocity in Core, m/s	0.531	0.531	0.529	0.515	0.479	0.455	0.342
Primary Coolant in Velocity in HX, m/s	0.395	0.395	0.394	0.384	0.357	0.339	0.255
Intermediate Coolant Velocity in HX, m/s	0.455	0.455	0.454	0.447	0.426	0.411	0.337
Intermediate Coolant Velocity in SG, m/s	0.299	0.299	0.299	0.294	0.281	0.271	0.222
Primary Coolant Temperature Rise, °C	140	140	141	145	156	164	219
Intermediate Coolant Temperature Rise, °C	137	137	137	139	146	152	186
Primary Coolant Outlet Temperature, °C	540	540	541	545	556	564	619
Intermediate Coolant Temperature at Top of HX, °C	494	494	494	497	505	511	551
Intermediate Coolant Temperature at Bottom of HX, °C	357	357	357	358	359	360	366
Primary-to-Intermediate Coolant Temperature Difference at Top of HX, °C	46.6	46.6	46.7	47.8	50.6	52.7	67.4
Primary-to-Intermediate Coolant Temperature Difference at Bottom of HX, °C	43.0	43.0	42.9	42.4	41.2	40.3	34.1

The ENHS involves flow through channels having hydraulic diameters of significantly differing sizes. A roughness grain of 10  $\mu\text{m}$  is nominally assumed as representative of an oxide film in Equation 6. As observed from Table 5, the calculated primary and intermediate temperature rises for NLP4 with LBE are about 5 and 2  $^{\circ}\text{C}$  greater, respectively, than would be obtained for a hydraulically smooth channel that corresponds to roughness sizes less than 1  $\mu\text{m}$ . An increase in the effective roughness grain size to 50  $\mu\text{m}$  would increase the temperature rises for NLP4 by another 11 and 7  $^{\circ}\text{C}$ , respectively, relative to the values at 10  $\mu\text{m}$ .

## SUMMARY

Natural circulation of the primary and intermediate coolants, or natural circulation enhanced by noncondensable gas injection, can be relied upon to transport the nominal core power from the core to the heat exchanger and from the heat exchanger to the steam generators. Primary coolant temperature rises and outlet temperatures are less than or equal to 160  $^{\circ}\text{C}$  and 560  $^{\circ}\text{C}$ , respectively. Intermediate coolant temperature rises and outlet temperatures are less than or equal to 141  $^{\circ}\text{C}$  and 519  $^{\circ}\text{C}$ , respectively. Very small differences in temperatures are calculated between lead-bismuth eutectic and lead coolants ( $\leq 2$   $^{\circ}\text{C}$  for temperature rises). With the exception of LP6, primary-to-intermediate coolant bulk temperature drops are less than or equal to 50  $^{\circ}\text{C}$ .

Uncertainties in thermophysical properties have a relatively small influence upon calculated best estimate primary and intermediate coolant system temperatures. The greatest uncertainty in the thermophysical properties is the uncertainty in compressibility,  $\beta$ . Uncertainty in  $\beta$  could increase the temperature rises by 6  $^{\circ}\text{C}$  above values calculated using ENHS team consensus properties. Other uncertainties in properties could further increase the temperature rises to a total of 9  $^{\circ}\text{C}$  above the values calculated using ENHS team consensus properties. Increase in roughness grain size from 10 to 50 microns could increase primary and intermediate coolant temperature rises by another 11 and 7  $^{\circ}\text{C}$ , respectively.

## ACKNOWLEDGMENTS

This work was funded under the U.S. Department of Energy 2001 NERI Program. The author is indebted to Professor Ehud Greenspan of the University of California at Berkeley and Dr. David C. Wade of Argonne National Laboratory for their support and encouragement.

## REFERENCES

1. E. Greenspan, N. W. Brown, M. D. Carelli, L. Conway, M. Dzodzo, Q. Hossain, D. Saphier, J. J. Sienicki, and D. C. Wade, "The Encapsulated Nuclear Heat Source A Generation IV Reactor," Proceedings of GLOBAL-2001, Paris, France, September 9-13, 2001.
2. E. Greenspan, N. W. Brown, M. D. Carelli, L. Conway, M. Dzodzo, Q. Hossain, D. Saphier, J. J. Sienicki, and D. C. Wade, "The Encapsulated Nuclear Heat Source Reactor for Proliferation-Resistant Nuclear Energy," Proceedings of GLOBAL-2001, Paris, France, September 9-13, 2001.
3. E. Greenspan, H. Shimada, D. C. Wade, M. D. Carelli, L. Conway, N. W. Brown, and Q. Hossain, "The Encapsulated Nuclear Heat Source Reactor Concept," ICONE-8750, Proceedings of ICONE-8, 8<sup>th</sup> International Conference on Nuclear Engineering, Baltimore, April 2-6, 2000.
4. J. J. Sienicki and D. C. Wade, "Thermal Hydraulic Analysis of the Encapsulated Nuclear Heat Source," ICONE-9771, Proceedings of ICONE-9, 9<sup>th</sup> International Conference on Nuclear Engineering, Nice, France, April 8-12, 2001.
5. H. Schlichting, Boundary Layer Theory, Fourth Edition, McGraw-Hill Book Company, Inc. New York (1960).
6. O. E. Dwyer, "Liquid-Metal Heat Transfer," Chapter 2 of Sodium-NaK Engineering Handbook Volume II Sodium Flow, Heat Transfer, Intermediate Heat Exchangers, and Steam Generators, ed. O. J. Foust, Gordon and Breach, Science Publishers, Inc., New York (1976).
7. S. A. Been, H. S. Edwards, C. E. Teeter, Jr., and V. P. Calkins, "The Densities of Liquids at Elevated Temperature: I. The Densities of Lead, Bismuth, Lead-Bismuth Eutectic, and Lithium in the Range Melting Point to 1000 $^{\circ}\text{C}$  (1832 $^{\circ}\text{F}$ )," NEPA 1585, Fairchild Engine and Airplane Corporation, NEPA Division (September 7, 1950).
8. N. A. Nikol'skii, N. A. Kalakutskaya, I. M. Pchelkin, T. F. Klassen, and V. A. Vel'tishcheva, "Thermal and Physical Properties of Molten Metals and Alloys," Problems of Heat Transfer, ed. M. A. Mikheev, Academy of Sciences, SSSR, Moscow (1995), translated into English as AEC-tr-4511.
9. J. K. Fink, "Pb-Bi Viscosity, Preliminary Recommendation," Available at [www.insc.anl.gov](http://www.insc.anl.gov).
10. J. Saar and H. Ruppertsberg, "Calculation of Cp(T) for Liquid Li/Pb Alloys from Experimental  $\rho(T)$  and  $(\partial P/\partial T)_s$  Data," Journal of Physics F Metal Physics, Vol. 17, p. 305 (1987).
11. A. F. Crawley, "Densities of Liquid Metals and Alloys," International Metallurgical Reviews, Vol. 19, p. 32 (1974).
12. J. K. Fink, "Enthalpy and Heat Capacity of Solid and Liquid Lead, Recommendations," Available at [www.insc.anl.gov](http://www.insc.anl.gov).